Cavity Ring-Down Spectroscopic Study of the Reactions of Br Atoms and BrO Radicals with Dimethyl sulfide

Yukio Nakano, Masashi Goto, Satoshi Hashimoto, and Masahiro Kawasaki*

Department of Molecular Engineering, Kyoto University, Kyoto 606-8501, Japan

Timothy J. Wallington

Ford Motor Company, SRL-3083, P.O. Box 2053, Dearborn, Michigan 48121-2053

Received: June 19, 2001; In Final Form: September 26, 2001

The title reactions were studied using cavity ring-down spectroscopy in 100 Torr of N_2 diluent at 278−333 K. The equilibrium constant and rates of the forward and reverse reactions of the Br + DMS ⇄ Br−DMS equilibrium were determined to be $K = (4.1 \pm 0.3) \times 10^{-15}$ cm^3 molecule^{-1}, $k_{forward} = (5.0 \pm 0.2) \times 10^{-11}$ cm^3 molecule^{-1} s^{-1}, and $k_{backward} = (1.2 \pm 0.2) \times 10^4$ s^{-1} at 300 K in 100 Torr of N_2. The absorption cross section of the Br−DMS adduct at 338.3 nm was $\sigma = (1.2 \pm 0.2) \times 10^{-17}$ cm^2 molecule^{-1}. An upper limit of $k < 1 \times 10^{-18}$ cm^3 molecule^{-1} s^{-1} was established for the reaction of O_2 with the Br−DMS adduct. The kinetics of the reaction of BrO with DMS were well described by the Arrhenius expression $k = (1.3 \pm 0.1) \times 10^{-14} \exp[(1033 \pm 265)/T]$ cm^3 molecule^{-1} s^{-1} ($k = 4.2 \times 10^{-13}$ cm^3 molecule^{-1} s^{-1} at 298 K). The uncertainties are 2 standard deviations from regression analyses.

1. Introduction

Dimethyl sulfide (DMS) is produced by phytoplankton in the oceans and is released into the atmosphere. DMS is the largest natural source of atmospheric sulfur.[1−5] Atmospheric oxidation of DMS is initiated by reaction with OH radicals during the daytime[6,7] and NO_3 radicals at night,[8−10] to give methanesulfonic acid (CH_3SO_3H), dimethyl sulfoxide (DMSO), dimethyl sulfone ($DMSO_2$), and sulfuric acid (H_2SO_4). The production of H_2SO_4 leads to the formation of cloud condensation nuclei. It has been proposed that DMS oxidation has a substantial impact on cloud formation over the oceans and hence influences the Earth's radiation balance and climate system.[11]

Interest in global climate change and the possible biological regulation of global climate has led to numerous studies of the atmospheric chemistry of DMS. However, despite a significant research effort, substantial uncertainties in our understanding of the atmospheric chemistry of DMS remain. Recent studies have shown that reactions of DMS with atomic halogens and halogen monoxide radicals can play roles in global halogen and sulfur cycles.[12] Unfortunately, uncertainties in the kinetic database for such reactions and in our understanding of the concentrations of atomic halogens and halogen monoxide radicals in marine air hinder our ability to quantify the importance of such reactions in the atmospheric chemistry of DMS.

In the present work, we concentrate on the reactions of DMS with bromine atoms and bromine monoxide radicals. At temperatures typical of the troposphere (<300 K), the reaction of Br atom with DMS proceeds via an association mechanism to form the Br−DMS adduct,[12−14] whereas at high temperatures (> 400 K), hydrogen atom abstraction is the dominant reaction pathway:[13]

$$Br + CH_3SCH_3 + M \rightleftarrows Br{-}DMS + M \qquad (1a,-1a)$$

$$Br + CH_3SCH_3 \rightarrow HBr + CH_3SCH_2 \qquad (1b)$$

Depending on the equilibrium constant for the reaction 1a,−1a and the reactivity of the Br−DMS adduct, it is conceivable that the Br−DMS adduct plays a significant role in the chemistry of marine air. There have been two experimental studies of the 1a,−1a equilibrium. Jefferson et al.[13] and Ingham et al.[15] employed laser flash photolysis with detection of Br atoms via resonance fluorescence and concluded that the Br−DMS adduct is sufficiently short-lived with respect to decomposition via reaction −1a and that this species is not important in atmospheric chemistry.

BrO radicals react with DMS to form Br atoms and dimethyl sulfoxide (DMSO):[16,17]

$$BrO + CH_3SCH_3 \rightarrow Br + CH_3S(O)CH_3 \qquad (2)$$

DMSO undergoes further oxidation to give aerosols and condensation nuclei. There have been three studies of the kinetics of reaction 2. Barnes et al.[16] and Bedjanian et al.[17] used discharge flow mass spectrocopy to study the reaction at low pressure in He diluent. Barnes et al.[16] reported a value of $k_2 = (2.7 \pm 0.5) \times 10^{-13}$ cm^3 molecule^{-1} independent of total pressure of He diluent over the range 0.5−3.6 mbar at 298 K. Bedjanian et al.[17] reported a value of $k_2 = (2.7 \pm 0.2) \times 10^{-13}$ cm^3 molecule^{-1} in approximately 1 Torr of He diluent at 297 K. Ingham et al.[15] used laser flash photolysis combined with UV absorption to monitor BrO radicals and reported $k_2 = (4.40 \pm 0.66) \times 10^{-13}$ cm^3 molecule^{-1} independent of total pressure of N_2 diluent over the range 60−200 Torr at 295 K. Barnes et al.,[16] Bedjanian et al.,[17] and Ingham et al.[15] observed that within the experimental uncertainties DMSO accounted for 100% of the loss of BrO radicals in the system. The kinetic data reported

* To whom correspondence should be addressed. E-mail: mkawasa7@ip.media.kyoto-u.ac.jp. Fax: +81-75-753-5526.

10.1021/jp012326f CCC: $20.00
Published on Web 11/09/2001

by Barnes et al.[16] and Bedjanian et al.[17] are in excellent agreement but are substantially lower than those reported by Ingham et al.[15]

Cavity ring-down spectroscopy (CRDS) is a new absorption spectroscopy technique based on measurement of the decay of a laser pulse confined within a cavity between two highly reflecting mirrors.[18−22] Spectroscopic and kinetic data are derived by measuring the increased rate of decay of the laser pulse caused by absorption in the cavity. The CRDS technique has been used in several kinetic studies[23−28] including our studies of BrO,[29] HCO,[30] and FCO[31] radicals. The sensitivity of CRDS enables low radical concentrations to be used, thus reducing potential complications caused by radical−radical reactions. In this study, we applied CRDS to study the kinetics of the reactions of Br and BrO with DMS and the UV absorption of the Br−DMS adduct. The goal of the present work is to provide further characterization of reactions 1 and 2 to facilitate their inclusion into global atmospheric chemistry models.

2. Experimental Section

The CRDS apparatus used in the present study is described in detail elsewhere.[29] The system employs two pulsed lasers. The first laser (either 355 or 266 nm output of Nd^{3+}:YAG laser, Spectra Physics GCR-250) was used to photolyze a suitable precursor to generate either Br atoms or BrO radicals. The second laser (Spectra Physics, PDL-3; LDS 698 Dye, pumped by the 532 nm output of a Nd:YAG laser Quantel Brilliant β) was used to probe the concentrations of reactive species in the system. The probe laser beam was frequency doubled by a KDP crystal and injected through one of two high-reflectivity mirrors which made up the ring-down cavity. The mirrors (Research Electro Optics) had a specified maximum reflectivity of 0.9995 at 350 nm, a diameter of 7.8 mm, and a radius of curvature of 1 m and were mounted 1.04 m apart. Light leaking from one of the mirrors of the ring-down cavity was detected by a photomultiplier tube (Hamamatsu, R212UH) through a broad band-pass filter (Toshiba, UVD33S). The decay of the light intensity was recorded using a digital oscilloscope (Tektronix, TDS430A) and transferred to a personal computer. The decay of the light intensity is given by eq I:

$$I(t) = I_0 \exp(-t/\tau) = I_0 \exp(-t/\tau_0 - \sigma nc(L_R/L)t) \quad \text{(I)}$$

where I_0 and $I(t)$ are the intensities of light at time 0 and t, respectively. τ_0 is the empty cavity ring-down time (5 μs at 338.3 nm). L_R is the length of the reaction region (0.55 m). L is the cavity length (1.04 m). τ is the measured cavity ring-down time. n and σ are the concentration and absorption cross section of the species of interest, and c is the velocity of light.

The reaction cell consisted of a Pyrex glass tube (21 mm i.d.), which was evacuated by a combination of an oil rotary pump and a mechanical booster pump. The temperature of the gas flow region was controlled by circulation of a thermostated mixture of ethylene glycol and water and was controllable over the range of 275−325 K. The difference between the temperature of sample gas at the entrance and exit of the flow region was <1 K. The pressure in the cell was monitored by an absolute pressure gauge (Baratron). Gas flows were measured and regulated by mass flow controllers (KOFLOC, 3650). A slow flow of nitrogen diluent gas was introduced at both ends of the ring-down cavity close to the mirrors to minimize deterioration caused by exposure to reactants and products. The total flow rate was kept constant at 1.0×10^3 cm^3 min^{-1} (STP). Ozone was produced by a silent electrical discharge in oxygen gas flow and was measured upstream of the reaction tube by monitoring the absorption at 253.7 nm ($\sigma = 6.86 \times 10^{-18}$ cm^2 molecule^{-1})[32] using a low-pressure Hg lamp as the light source. The concentration of DMS was measured upstream of the reaction tube by monitoring absorption of the 213.9 nm ($\sigma = 1.7 \times 10^{-18}$ cm^2 molecule^{-1}) output of a zinc hollow cathode lamp.[33]

In the study of the Br + DMS reaction, Br atoms were generated by the 355 nm photolysis of Br_2 ($(8-20) \times 10^{13}$ molecule cm^{-3}). Br($^2P_{1/2}$) atoms are rapidly relaxed to Br($^2P_{3/2}$) by collision with N_2.[34] The initial Br atom concentration was determined by titration with excess O_3 ($(4-8) \times 10^{18}$ molecule cm^{-3}) and measurement of the resulting BrO concentration.[29] Br($^2P_{3/2}$) atoms react with DMS to give the Br−DMS adduct which has a broad absorption band in the region from 300 to 450 nm.[15] In the present work, the Br−DMS adduct was monitored using its absorption at 338.3 nm. The CRD decay curves were measured at two different wavelengths, one corresponds to the peak position of the BrO absorption (Ia) and the other at the valley position (Ib). By the subtraction of Ib from Ia, the contribution of BrO is obtained. The Br−DMS adduct undergoes rapid decomposition, and an equilibrium is established given by reaction 1a,−1a. Temporal changes in the concentration of the Br−DMS adduct were used to determine the rate constant k_{1a}, equilibrium constant $K_{1a} = k_{1a}/k_{-1a}$, and absorption cross section of the Br−DMS adduct.

In the study of the BrO + DMS reaction, BrO radicals were produced by the 266 nm photolysis of O_3 (typically 4×10^{12} molecule cm^{-3}) in the presence of Br_2 ($(4-40) \times 10^{13}$ molecule cm^{-3}) in N_2 diluent at 100 Torr. O(^{1}D) and O(^{3}P) atoms are generated by the photolysis of O_3. O(^{1}D) atoms are rapidly relaxed to O(^{3}P) by collision with N_2. O(^{3}P) atoms react with Br_2 to produce BrO radicals which then react with DMS in reaction 2. BrO radicals were monitored using their characteristic absorption at 338.5 nm ($A^2\Pi_{3/2}-X^2\Pi_{3/2}$ (7,0) band[29]). The decay of BrO radicals in the presence of excess DMS was used to provide kinetic data for the BrO + DMS reaction. Experiments were performed in 100−200 Torr of N_2, or 100 Torr of SF_6, diluent. Uncertainties reported herein are 2 standard deviations unless otherwise stated.

All reagents were obtained from commercial sources. Br_2 (99.0%) and DMS (98.0%) were subjected to repeated freeze−pump−thaw cycling before use. N_2 (>99.999%), O_2 (>99.995%), and SF_6 (>99.99%) were used without further purification.

3. Results

3.1. Kinetics of the Reaction of Br with DMS. By measuring the concentration of BrO radicals produced following the laser flash photolysis of $Br_2/O_3/N_2$ mixtures,[29] the initial Br atom concentration in the present set of experiments, $[Br]_0$, was determined to be $(0.4-2) \times 10^{12}$ molecule cm^{-3}:

$$Br + O_3 \rightarrow BrO + O_2$$
$$k_3 = 1.7 \times 10^{-11} \exp(800/T) \text{ cm}^3 \text{ molecule}^{-1} \text{ s}^{-1} \quad (3)$$

Following the generation of Br atoms in gas mixtures containing $(0.3-3.2) \times 10^{14}$ molecule cm^{-3} of DMS in 100 Torr of N_2 diluent, a rapid increase in absorption at 338.3 nm was observed (see Figure 1). This absorption is attributed to the formation of the Br−DMS adduct which absorbs strongly in the region of 300−450 nm.[15]

The rate of increase in this absorption contains information concerning the kinetics of reaction 1a. Diffusion of Br−DMS adduct from the detection region can be ignored over the short experimental time scale (10−200 ms). The DMS concentration

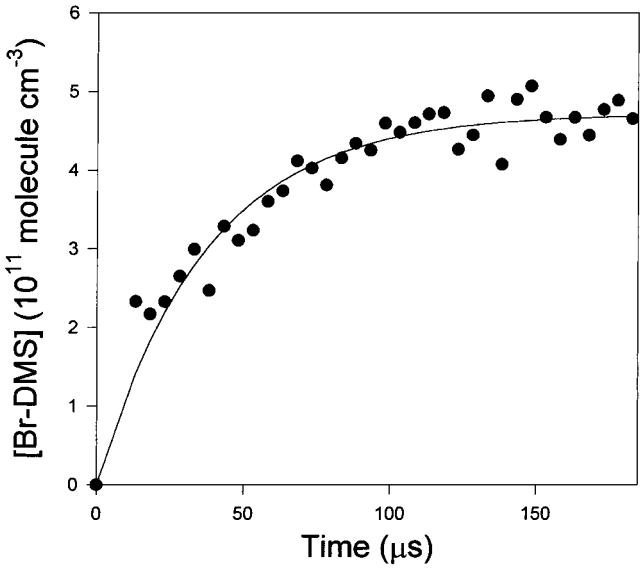

Figure 1. Pseudo-first-order rise of the Br−DMS adduct in 100 Torr of N_2 diluent at 300 K. The curve line is a fit of eq II to the data. $[CH_3SCH_3] = 3.2 \times 10^{14}$ molecule cm^{-3}; $[Br]_0 = 8.3 \times 10^{11}$ molecule cm^{-3}.

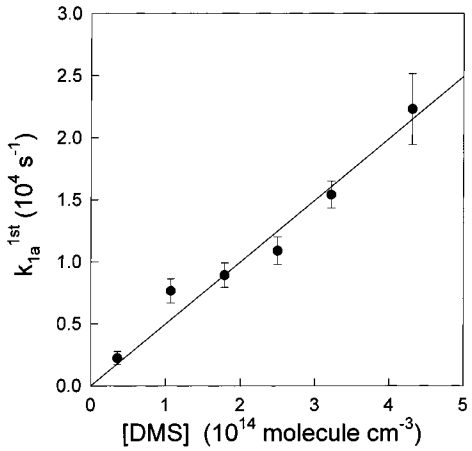

Figure 2. Second-order plot for the reaction of Br with DMS in 100 Torr of N_2 at 300K. The line is a linear least-squares fit.

was in great excess over that of Br atoms, and the rise of absorption attributable to the Br−DMS adduct followed pseudo-first-order kinetics. According to reaction 1a, the formation of the Br−DMS adduct can be analyzed using the following equations:

$$[\text{Br−DMS}]_t = [\text{Br}]_0\{K_{1a}[\text{DMS}]/(K_{1a}[\text{DMS}] + 1)\}\{1 - \exp(-k_{1a}^{1st} - (k_{1a}^{1st}/K_{1a}[\text{DMS}])t)\} \quad \text{(II)}$$

$$k_{1a}^{1st} = k_{1a}[\text{DMS}] \quad \text{(III)}$$

where $[\text{Br−DMS}]_t$ is the concentration of Br−DMS at time t and $[\text{Br}]_0$ is the concentration of Br at time 0. k_{1a} and k_{1a}^{1st} are the second order and pseudo-first-order rate constants for reaction 1a, respectively. The equilibrium constants $K_{1a} = k_{1a}/k_{-1a}$ at various temperatures and the absorption cross section of the Br−DMS adduct at 338.3 nm are described in the following section. Figure 2 shows a plot of k_{1a}^{1st} versus [DMS] for experiments conducted at room temperature in a total pressure of 100 Torr of N_2 diluent. The second-order rate constant k_{1a} is obtained from a linear least-squares analysis of the data in Figure 2: $k_{1a} = (5.0 \pm 0.2) \times 10^{-11}$ cm^3 molecule^{-1} s^{-1} at 300 K.

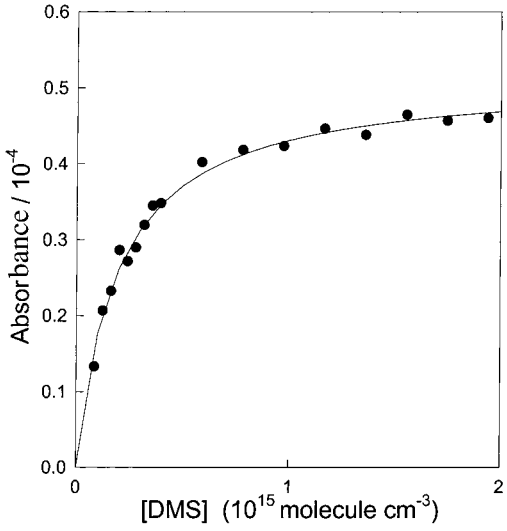

Figure 3. Absorbance of the Br−DMS adduct at 338.3 nm as a function of [DMS]. The solid line is a fit of eq IV to the data.

Following addition of Br atoms to DMS to produce the Br−DMS adduct, the reaction system reaches an equilibrium given by reaction 1a,−1a. Figure 3 shows the absorbance at 338.3 nm of the Br−DMS adduct at equilibrium versus the concentration of DMS used in the experiment ($(1-20) \times 10^{14}$ molecule cm^{-3}) for experiments conducted at 300 K. As expected, the equilibrium concentration of the Br−DMS adduct increased with increasing DMS concentration and tended toward a limiting value reflecting the condition where essentially all of the Br atoms are associated with DMS. The dependence of the absorption at equilibrium on [DMS] can be expressed by eq IV:

$$A = \sigma(\lambda)L_R K_{1a}[\text{Br}]_0[\text{DMS}]_{eq}/(1 + K_{1a}[\text{DMS}]_{eq}) \quad \text{(IV)}$$

where A and $\sigma(\lambda)$ are absorbance and absorption cross section of Br−DMS adduct at wavelength $\lambda = 338.3$ nm, respectively. K_{1a} is an equilibrium constant of the reaction 1a,−1a. L_R is the effective path length, and $[\text{Br}]_0$ is the initial Br atom concentration (determined via titration with ozone in a separate experiment). Dimethyl sulfide is in large excess, and its concentration at equilibrium is essentially the same as that measured prior to generation of Br atoms in the reaction vessel.

Figure 3 shows a fit of eq IV to the data with $\sigma(\lambda)$ and K_{1a} varied simultaneously to provide the best fit. As seen from Figure 3, eq IV provides a good description of the data trend. The least squares regression analysis provides values of $K_{1a} = (4.1 \pm 0.3) \times 10^{-15}$ cm^3 molecule^{-1} and σ(Br−DMS, 338.3 nm) $= (1.2 \pm 0.2) \times 10^{-17}$ cm^2 at 300 K in 100 Torr of N_2 diluent, which can be compared to the cross-section $(2.74^{+1.6}_{-1.1}) \times 10^{-17}$ cm^2, reported by Ingham et al.[15] The rate constant for the back reaction, Br + Br−DMS, was reported to be 4.2×10^{-10} cm^3 molecule s^{-1} by Ingham et al.[15] With a kinetics simulation program, we found that the equilibrium for the adduct formation is achieved first, and then, the adduct is lost slowly by attack of Br. Thus, the absolute concentrations of the BrDMS complex were estimated with eq IV.

Equilibrium constants, K_{1a}, were measured at various temperatures over the range of 275−325 K and are given in Table 1. The van't Hoff plot of $\ln(K_{1a}[\text{M}])$ versus the inverse of temperature is shown in Figure 4. The enthalpy change, ΔH, and entropy change, ΔS, in the equilibrium reaction 1a,−1a were determined using eq V:

$$\ln(K_{1a}[\text{M}]) = -\Delta H/RT + \Delta S/R \quad \text{(V)}$$

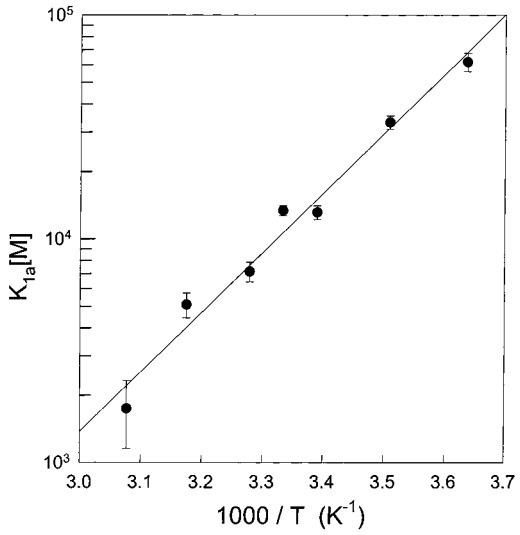

Figure 4. van't Hoff plot for the equilibrium 1a,−1a; Br + DMS ⇄ Br−DMS adduct.

TABLE 1: Values of the Br + DMS ⇄ Br−DMS Equilibrium Constant Measured in the Present Work in 100 Torr of N_2 Diluent

temp (K)	K_{1a} (10^{-15} cm^3 molecule^{-1})
275	19.2 ± 1.8
285	10.3 ± 0.7
295	4.08 ± 0.29
300	4.16 ± 0.22
305	2.22 ± 0.22
315	1.58 ± 0.20
325	0.54 ± 0.18

where [M] is a concentration of third body. R is the gas constant. By fitting eq V to the data in Figure 4, values of $\Delta H = -51 \pm 4$ kJ mol^{-1} and $\Delta S = -93 \pm 12$ J mol^{-1} K^{-1} were obtained. These values are in excellent agreement with the measurements by Jefferson et al.[13] ($\Delta H = -61 \pm 5$ kJ mol^{-1} and $\Delta S = -96 \pm 16$ J mol^{-1} K^{-1} measured at 334 K for 760 Torr). The Br−S bond is formed in reaction 1a, and the value of $\Delta H = -51 \pm 4$ kJ mol^{-1} is the Br−S bond strength in the Br−DMS adduct.

The value of $K_{1a} = (4.1 \pm 0.3) \times 10^{-15}$ cm^3 molecule^{-1} at 300 K can be combined with our determination of $k_{1a} = (5.0 \pm 0.3) \times 10^{-11}$ cm^3 molecule^{-1} s^{-1} to give the rate constant for unimolecular decomposition of the Br−DMS adduct at 300 K; $k_{-1a} = (1.2 \pm 0.2) \times 10^4$ s^{-1}. This result is consistent with the value of $k_{-1a} = (1.02 \pm 0.07) \times 10^4$ s^{-1} at 295 K in 100 Torr of N_2 reported recently by Ingham et al.[15]

The rapid unimolecular decomposition of the Br−DMS adduct reflects the weakness of the Br−S bond (51 ± 4 kJ mol^{-1}). It is interesting to contrast the instability of the Br−DMS adduct to the relative stability of the Cl-DMS adduct which does not show any evidence of decomposition on the millisecond time scale.[35] The experimental data indicate that the Cl-DMS bond is considerably stronger than the Br−DMS bond.[35] There have been three computational determinations of the Cl-DMS bond strength.[36−38] McKee[36] and Resende and De Almeida[37] calculated Cl−S bond strengths of 51.0 and 51.5 kJ mol which are indistinguishable from the experimental data for the Br−S bond strength in the Br−DMS adduct. In contrast, Wilson and Hirst[38] report a value of 80.9 kJ mol for the Cl−S bond which is significantly greater than that of the Br−S bond. It appears that Cl-DMS bond strength has been underestimated in the work of McKee[36] and Resende and De Almeida.[37]

The value of $k_{-1a} > (1.4 \pm 0.2) \times 10^4$ s^{-1} measured herein in 100 Torr total pressure can be used to estimate an upper limit for the lifetime of the Br−DMS adduct with respect to thermal decomposition in one atmosphere of air at ambient temperature of 70 ms. The only atmospheric species capable of scavenging the Br−DMS adduct on a time scale competitive with reaction −1a is O_2:

$$\text{Br−DMS} + O_2 \rightarrow \text{DMSO} + \text{BrO} \qquad (4)$$

To search for BrO production from reaction 4, experiments using the 355 nm photolysis of Br_2 in DMS/O_2 mixtures were performed. However, generation of BrO radicals was not observed with our CRDS study (maximum detection limit is 5×10^{10} cm^{-3}). These results indicate that the Br−DMS adduct is not reactive toward O_2. Using the detection limit for BrO (5×10^{10} cm^{-3}), the concentration of Br−DMS adduct (2.7×10^{12} cm^{-3}) and O_2 (3.2×10^{18} cm^{-3}), and the first-order decay rate constant of BrO (200 s^{-1}) via diffusion and reaction with DMS, an upper limit value of $k_4 < 1 \times 10^{-18}$ cm^3 molecule^{-1} s^{-1} was determined. In one atmosphere of air, the pseudo first-order loss of Br−DMS adduct with respect to reaction with O_2 is <5 s^{-1}. The atmospheric fate of the Br−DMS adduct is decomposition via reaction −1a.

3.2. Kinetics of the Reaction of BrO with DMS. BrO radicals were produced by the 266 nm photolysis of O_3 in the presence of Br_2 at a total pressure of 100 Torr with N_2 diluent at temperatures of 278−333 K in the presence of DMS ($(4-40) \times 10^{13}$ molecule cm^{-3}). Under these conditions, BrO radicals are lost via reaction with DMS and via self-reaction:[27]

$$2\text{BrO} \rightarrow 2\text{Br} + O_2 \qquad k_{5a} = 2.4 \times 10^{-12} \exp(40/T) \text{ cm}^3 \text{ molecule}^{-1} \text{ s}^{-1} \qquad (5a)$$

$$\rightarrow \text{Br}_2 + O_2 \qquad k_{5b} = 2.8 \times 10^{-14} \exp(860/T) \text{ cm}^3 \text{ molecule}^{-1} \text{ s}^{-1} \qquad (5b)$$

Assuming that BrO radicals are lost via reactions 2, 5a, and 5b and diffusion from the detection region, the decay of BrO can be analyzed as a sum of first- and second-order kinetics using eq VI:

$$\frac{1}{[\text{BrO}]_t} = \left\{\left(\frac{1}{[\text{BrO}]_0} + \frac{2k_5}{k_2^{1st}}\right)\exp(k_2^{1st}t) - \left(\frac{2k_5}{k_2^{1st}}\right)\right\} \qquad (VI)$$

where $[\text{BrO}]_t$ and $[\text{BrO}]_0$ are the concentrations of BrO at time t and 0, respectively. k_5 is the rate constant of reactions 5a and 5b ($k_5 = k_{5a} + k_{5b}$). k_2^{1st} is the sum of the pseudo-first-order rate losses of BrO radicals via reaction 2 and diffusion from the detection region:

$$k_2^{1st} = k_2[\text{DMS}] + k_d \qquad (VII)$$

The regeneration reaction of BrO from Br + O_3 is slow under our experimental conditions (typical time scale for BrO regeneration was a few hundred ms). Because of the high concentration of CH_3SCH_3, the following successive reactions of Br were considered:

$$\text{BrO} + \text{DMS} \rightarrow \text{Br} + \text{DMSO} \qquad (2)$$

$$\text{Br} + \text{DMS} \rightarrow \text{Br−DMS} \qquad (1a)$$

$$\text{Br−DMS} + \text{Br} \rightarrow \text{Br}_2 + \text{DMS} \qquad (6)$$

Even with $k_6 = 4.2 \times 10^{-10}$ cm^3 molecule s^{-1} reported by Ingham et al.,[15] eq VI is applicable under our experimental

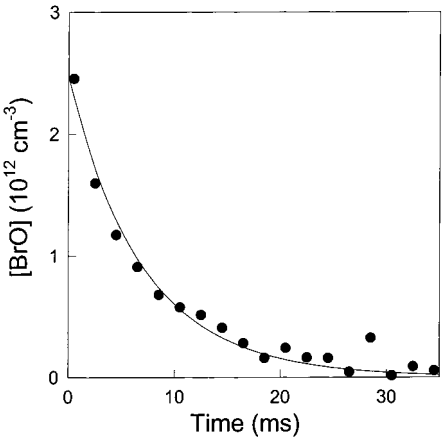

Figure 5. Pseudo-first-order decay profile of BrO. The curve is a fit of eq VI to the data in 100 Torr of N_2 diluent at 300 K. P(N_2) = 100 Torr; [CH_3SCH_3] = 3.7 × 10^{14} molecule cm^{-3}; [O_3]$_0$ = 4 × 10^{12} molecule cm^{-3}.

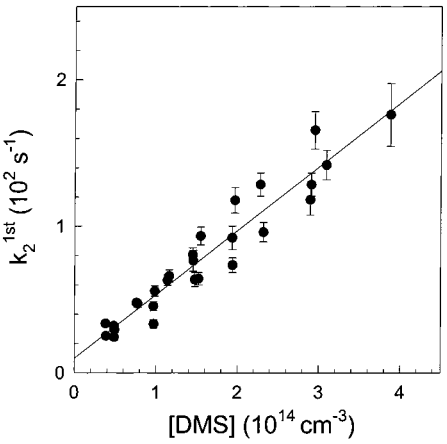

Figure 6. Second-order plot for the reaction of BrO with DMS in 100 Torr of N_2 diluent at 300K. The line is a linear least-squares fit.

conditions, that is, under relatively low radical concentrations. Figure 5 shows an example of the temporal profile of BrO and a fit of eq VI to the data. Figure 6 shows k_2^{1st} versus [DMS] in 100 Torr of N_2 diluent at 300 K, linear least-squares analysis gives $k_2 = (4.6 \pm 0.6) \times 10^{-13}$ cm^3 molecule^{-1} s^{-1}. This result is in excellent agreement with the finding of Ingham et al.[15] that $k_2 = (4.4 \pm 0.7) \times 10^{-13}$ cm^3 molecule^{-1} s^{-1} at 295 K.

The aim of the present work was to provide kinetic data for reaction 2 suitable for inclusion into atmospheric models. The question arises as to whether a value of k_2 obtained in 100 Torr of N_2 diluent provides a good description of the kinetics in 760 Torr of air diluent. To test for an effect of the nature or total pressure of diluent gas, additional experiments were performed using 100 Torr of SF_6 or 200 Torr of N_2 diluent which gave values of $k_2 = (4.5 \pm 0.3) \times 10^{-13}$ and $(4.5 \pm 0.8) \times 10^{-13}$ cm^3 molecule^{-1} s^{-1}, respectively. The insensitivity of k_2 to the nature and pressure of diluent gas suggests that values of k_2 determined in 100 Torr of N_2 are appropriate for use in atmospheric models. This conclusion is consistent with the observation of Ingham et al.,[15] that there was no effect of total pressure over the range 60−200 Torr of N_2 diluent.

To determine the Arrhenius expression for the reaction of BrO with DMS, rate constants of reaction 2 were measured at various temperatures (278−333 K). The results are listed in Table 2 and plotted in Figure 7. Linear least-squares analysis of the data in Figure 7 gives $k_2 = (1.3 \pm 0.1) \times 10^{-14}$ exp[$(1033 \pm 265)/T$] cm^3 molecule^{-1} s^{-1}. The negative activation

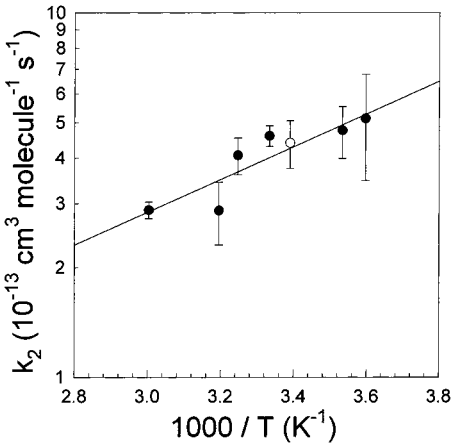

Figure 7. Arrhenius plot for the reaction of BrO with DMS. Present work (closed circle) and Ingham et al. of ref 15 (open circle).

TABLE 2: Values of the Rate Constant of the BrO + DMS Reaction Measured in the Present Work in 100 Torr of N_2 Diluent

temp (K)	k_2 (10^{-13} cm^3 molecule^{-1} s^{-1})
278	5.13 ± 1.66
283	4.76 ± 0.77
300	4.60 ± 0.60
308	4.07 ± 0.47
313	2.87 ± 0.56
333	2.88 ± 0.15

energy ($E_a = -8.6 \pm 2.2$ kJ mol^{-1}) determined herein is consistent with that determined in the low pressure study of Bedjanian et al.[17] ($E_a = -7.0 \pm 1.5$ kJ mol^{-1}). However, the absolute values of k_2 measured herein are substantially greater (by 50% at ambient temperature) than the values reported by Bedjanian et al.[17] The negative activation energy suggests that the reaction of BrO with DMS proceeds via an associated complex as shown below:

$$\mathrm{BrO + DMS \rightleftarrows [BrO{-}DMS] \rightarrow Br + DMSO} \qquad (2)$$

As discussed above, the available experimental data suggest that the Arrhenius expression derived in this work from experiments conducted in 100 Torr of N_2 diluent is appropriate for representing the kinetics of this reaction at atmospheric pressure. Consequently, we recommend use of $k_2 = (1.3 \pm 0.1) \times 10^{-14}$ exp[$(1033 \pm 265)/T$] cm^3 molecule^{-1} s^{-1} in global atmospheric models.

4. Atmospheric Implications

The equilibrium constant for the Br−DMS adduct K_{1a} determined here can be combined with an estimate of [Br] = 5 × 10^5 molecule cm^{-3} and a typical value of [DMS] = 5 × 10^9 molecule cm^{-3} to derive an estimate of 10 molecule cm^{-3} for the concentration of the Br−DMS adduct in the marine boundary layer.[39,40] This extremely small concentration combined with the fact that the adduct does not react rapidly with O_2 renders the Br−DMS adduct of essentially no importance in atmospheric chemistry.

The present study is the first study of the kinetics of the BrO + DMS reaction as a function of temperature at high pressure. It was determined that $k_2 = (4.6 \pm 0.6) \times 10^{-13}$ cm^3 molecule^{-1} s^{-1} in 100 Torr of N_2 at 300 K. This result is approximately 1.8 times greater than the NASA data panel's recommendation[32] of $k_2 = 2.6 \times 10^{-13}$ cm^3 molecule^{-1} s^{-1} which was based upon the low-pressure data of Barnes et al.[16] and Bedjanian et al.[17] However, our result is in an excellent agreement with that

reported recently by Ingham et al.,[15] $k_2 = (4.4 \pm 0.6) \times 10^{-13}$ cm^3 molecule^{-1} s^{-1} in 60−200 Torr of N_2 diluent at 295 K. It appears that previous measurements carried out at low pressures (<4 Torr of He) do not provide a reliable measure of the kinetics of the BrO + DMS reaction under atmospheric conditions.

The kinetic data for the BrO + DMS reaction measured herein support and extend (to temperatures other than ambient) the recent findings of Ingham et al.[15] The present work taken together with that of Ingham et al.[15] provides compelling evidence that the values of k_2 used in present global atmospheric models are too low by approximately a factor of 1.8. Ingham et al.[15] used a chemical box model (MOCCA[40,41]) to assess the importance of reaction 2 in the atmospheric chemistry of DMS. The MOCCA model provides a detailed description of the loss of DMS via reaction with OH, NO_3, Cl, Br, BrO, and IO radicals in the marine boundary layer. Using their value of $k_2 = (4.4 \pm 0.7) \times 10^{-13}$ cm^3 molecule^{-1} s^{-1} at 295 K, Ingham et al.[15] found that incorporation of reaction 2 into the MOCCA model lead to a decrease in [DMS] by approximately a factor of 2 and an increase in [DMSO] by approximately a factor of 4. It is clear that reaction with BrO radicals is an important sink for DMS and an important source of DMSO in marine environments. As seen in Figure 7, the results from the present work show that reaction 2 has a negative temperature dependence given by $k_2 = (1.3 \pm 0.1) \times 10^{-14} \exp[(1033 \pm 265)/T]$ cm^3 molecule^{-1} s^{-1}. Use of this expression in the MOCCA model would increase the importance of reaction 2 slightly (by approximately 10%) over that reported by Ingham et al.[15]

Finally, it should be noted that BrO radicals are regenerated by reaction of Br atoms with ozone and hence reaction 2 will not decrease the level of BrO radicals in the atmosphere:

$$\mathrm{BrO} + \mathrm{DMS} \rightarrow \mathrm{Br} + \mathrm{DMSO}$$
$$\mathrm{Br} + \mathrm{O_3} \rightarrow \mathrm{BrO} + \mathrm{O_2}$$

Ozone is present in the marine boundary layer at a concentration which is typically 1000 times greater than that of DMS. Although reaction 2 is an important loss mechanism for DMS it is not an important loss mechanism for ozone.

Acknowledgment. The authors thank Mr. Shinji Nakamichi for his help with the experiments. This work was supported by a Grant-in-Aid for the priority research field "Radical Reactions" from the Ministry of Education, Japan, and a NEDO International Joint Research Grant.

References and Notes

(1) Cullis, C. F.; Hirschler, M. M. *Atoms. Environ.* **1980**, *14*, 1263.

(2) Andreae, M. O.; Ferek, R. J.; Bermond, F.; Byrd, K. P.; Engstrom, R. T.; Hardin, S.; Houmere, P. D.; Le Marrec, F.; Raemdonck, H.; Chatfield, R. B. *J. Geophys. Res.* **1985**, *90*, 12891.

(3) Bates, T. S.; Lamb, B. K.; Guenther, A.; Dignon, J.; Stoiber, R. E. *J. Atmos. Chem.* **1992**, *14*, 315.

(4) Kettele, A. J.; Andreae, M. O. *J. Geophys. Res.* **2000**, *105*, 2679.

(5) Shon, Z. H.; Davis, D.; Chen, G.; Grodzinsky, G.; Bandy, A.; Thornton, D.; Sandholm, S.; Bradshaw, J.; Stickel, R.; Chameides, W.; Kok, G.; Russell, L.; Mauldin, L.; Tanner, D.; Eisele, F. *Atoms. Environ.* **2001**, *35*, 159.

(6) Tyndall, G. S.; Ravishankara, A. R. *Int. J. Chem. Kinet.* **1991**, *23*, 483.

(7) Sekušak, S.; Piecuch, P.; Bartlett, R. J.; Cory M. G. *J. Phys. Chem. A* **2000**, *104*, 8779.

(8) Cooper, D. J. *J. Atoms. Chem.* **1996**, *25*, 97.

(9) Ravishankara, A. R.; Rudich, Y.; Talukdar, R.; Barone, S. B. *Philos. Trans. R. Res. London Ser. B* **1997**, *352*, 171.

(10) Allan, B. J.; McFiggans, G.; Plane, J. M. C.; Coe, H.; McFadyen, G. G. *J. Geophys. Res.* **2000**, *105*, 24191.

(11) Charlson, R. J.; Lovelock, J. E.; Andreae, M. O.; Warren, S. G. *Nature* **1987**, *326*, 655.

(12) Barnes, I.; Becker, K. H.; Overath, R. D. In Tropospheric Chemistry of Ozone in the Polar Regions. *Global Environmental Change*; NATO ASI Series 1; Niki, H., Becker, K. H., Eds.; 1993, I 7, 371.

(13) Jefferson, A.; Nicovich, J. M.; Wine, P. H. *J. Phys. Chem. A* **1994**, *98*, 7128.

(14) Wine, P. H.; Nicovich, J. M.; Stickel, R. E.; Zhao, Z.; Shackelford, C. J.; Kreutter, K. D.; Daykin, E. P.; Wang, S. In *Global Environmental Change*; NATO ASI Series 1; Niki, H., Becker, K. H., Eds.; 1993, I 7, 385.

(15) Ingham, T.; Bauer, D.; Sander, R.; Crutzen, P. J.; Crowley, J. N. *J. Phys. Chem. A* **1999**, *103*, 7199.

(16) Barnes, I.; Bastian, V.; Becker, K. H.; Overath, R. D. *Int. J. Chem. Kinet.* **1991**, *23*, 579.

(17) Bedjanian, Y.; Poulet, G.; LeBras, G. *Int. J. Chem. Kinet.* **1996**, *28*, 383.

(18) O'Keefe, A.; Deacon, D. D. G. *Rev. Sci. Instrum.* **1988**, *59*, 2544.

(19) Zalicki, P.; Zare, R. N. *J. Chem. Phys.* **1995**, *102*, 2708.

(20) Berden, G.; Peeters, R.; Meijer, G. *Int. Rev. Phys. Chem.* **2000**, *19*, 565.

(21) King, M. D.; Dick, E. M.; Simpson, W. R. *Atmos. Environ.* **2000**, *34*, 685.

(22) Tonokura, K.; Marui, S.; Koshi, M. *Chem. Phys. Lett.* **1999**, *313*, 771.

(23) Wheeler, N. D.; Newman, S. M.; Orr-Ewing, A. J.; Ashfold, M. N. R. *J. Chem. Soc., Faraday. Trans.* 1**998**, *94*, 337.

(24) Yu, T.; Lin, M. C. *J. Phys. Chem.* **1994**, *98*, 9697.

(25) Zhu, L.; Johnston, G. *J. Phys. Chem.* **1995**, *99*, 15114.

(26) Atkinson, D. B.; Hudgens, J. W. *J. Phys. Chem. A* **1997**, *101*, 3901.

(27) Brown, S. S.; Wilson, R. W.; Ravishankara A. R. *J. Phys. Chem. A* **2000**, *104*, 4976.

(28) Brown, S. S.; Ravishankara, A. R.; Stark, H. *J. Phys. Chem. A* **2000**, *104*, 7044.

(29) Ninomiya, Y.; Hashimoto, S.; Kawasaki, M.; Wallington, T. J. *Int. J. Chem. Kinet.* **2000**, *32*, 125.

(30) Ninomiya, Y.; Goto, M.; Hashimoto, S.; Kagawa, Y.; Yoshizawa, K.; Kawasaki, M.; Wallington, T. J.; Hurley, M. D. *J. Phys. Chem. A* **2000**, *104*, 7556.

(31) Ninomiya, Y.; Goto, M.; Hashimoto, S.; Kawasaki, M.; Wallington, T. *J. Int. J. Chem. Kinet.* **2001**, *33*, 130.

(32) DeMore, W. B.; Sander, S. P.; Golden, D. M.; Hampson, R. F.; Kurylo, M. J.; Howard, C. J.; Ravishankara, A. R.; Kolb, C. E.; Molina, M. J. *Chemical Kinetics and Photochemical Data for use in Stratospheric Modeling*, JPL Publication 97-4; Jet Propulsion Laboratory: Pasadena, CA, 1997.

(33) Hearn, C. H.; Turcu, E.; Joens, J. A. *Atmos. Environ.* **1990**, *24A*, 1939.

(34) Johnson, R. O.; Perram, G. P.; Roh W. B. *J. Chem. Phys.* **1996**, *104*, 7052.

(35) Urbanski, S. P.; Wine, P. H. *J. Phys. Chem. A* **1999**, *103*, 10935.

(36) McKee, M. L. *J. Phys. Chem.* **1993**, *97*, 10971.

(37) Resende, S. M.; De Almeida, W. B. *J. Phys. Chem. A* **1997**, *101*, 9738.

(38) Wilson, C.; Hirst, D. M. *J. Chem. Soc., Faraday Trans.* **1997**, *93*, 2831.

(39) Chin, M.; Jacob, D. J.; Gardner, G. M.; Foreman-Fowler, M. S.; Spiro, P. A.; Savoie, D. L. *J. Geophys. Res.* **1996**, *101*, 18667.

(40) Sander, R.; Crutzen, P. J. *J. Geophys. Res.* **1996** *101*, 9121.

(41) Vogt, R.; Crutzen, P. *Nature* **1996**, *383*, 327.